analytical chemistry

Article

Cite This: *Anal. Chem.* XXXX, XXX, XXX−XXX

pubs.acs.org/ac

Conductive Adhesive Film Expands the Utility of Matrix-Assisted Laser Desorption/Ionization Mass Spectrometry Imaging

Daisuke Saigusa,[*,†,‡,§] Ritsumi Saito,[†,‡] Komei Kawamoto,[∥] Akira Uruno,[†,‡] Kuniyuki Kano,[‡,⊥] Junken Aoki,[‡,⊥] Masayuki Yamamoto,[†,‡] and Tadafumi Kawamoto[*,∥]

[†]Department of Integrative Genomics, Tohoku Medical Megabank Organization, Tohoku University, 2-1 Seiryo-machi, Aoba-ku, Sendai, Miyagi 980-8573, Japan

[‡]Medical Biochemistry, Tohoku University School of Medicine, 2-1 Seiryo-machi, Aoba-ku, Sendai, Miyagi 980-8575, Japan

[§]LEAP, Japan Agency for Medical Research and Development (AMED), 1-7-1, Otemachi, Chiyoda-ku, Tokyo, Japan

[∥]School of Dental Medicine, Tsurumi University, 2-1-3 Tsurumi, Tsurumi-ku, Yokohama, Kanagawa 230-8501, Japan

[⊥]Laboratory of Molecular and Cellular Biochemistry, Graduate School of Pharmaceutical Sciences, Tohoku University, 6-3 Aoba, Aramaki-aza, Aoba-ku, Sendai, Miyagi 980-8578, Japan

Supporting Information

ABSTRACT: The matrix-assisted laser desorption/ionization mass spectrometry imaging (MALDI-MSI) technique is a promising approach for detecting the distribution of small molecules in a section of biological tissue. However, when a cryosection is created from fragile, hard, or whole-body samples, obtaining a high-quality section that maintains the distribution of the various components has been difficult. Since adhesive films have the potential to obtain high-quality cryosections, we attempted to utilize a conductive adhesive film for MALDI-MSI. To this end, cryosections of the whole body of a 9-day-old mouse were directly prepared on indium tin oxide (ITO) glass slides, nonconductive adhesive films, or conductive adhesive films, and the signal intensities from each section were measured by MALDI-MSI. We measured the differences in the ion intensity among these three slides/films by means of multivariate analyses and found that both the nonconductive and conductive adhesive films gave rise to high-quality sections in comparison with the ITO glass slide. The conductive adhesive film gave higher signals that were comparable to those of the ITO glass slide in comparison with the nonconductive adhesive film. We divided the frozen sections into two groups, a freeze-dried group and a thawed group, to examine the freeze−thaw effect on the signals of representative compounds of amino acids, cholesterol, and phosphatidylcholines. The freeze-dried samples were found to be useful for the analysis. These results indicate that the sections made with the conductive adhesive film under a freeze-dried condition can expand the utility of the MALDI-MSI analysis.

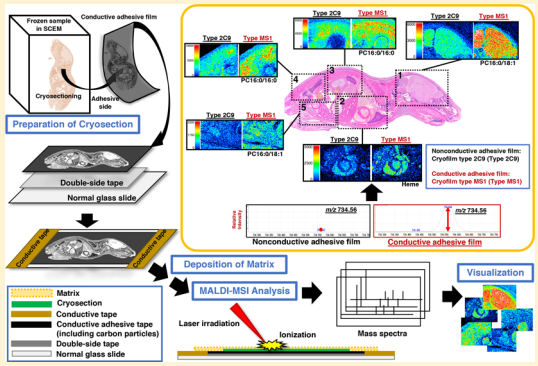

The matrix-assisted laser desorption/ionization mass spectrometry imaging (MALDI-MSI) technique is an important approach for observing the distribution of small molecules on the surfaces of section samples, including biological,[1,2] agriculture,[3,4] and insect samples.[5] The reproducibility and sensitivity of MALDI-MSI analyses have been improved by the development of stable techniques for applying a matrix in the process of sample preparation: for instance, the two-step deposition and spray method,[6−8] the spray and reclustering method,[9] sensitive detection methods using derivatization,[10,11] and addition of a salt.[12] In addition, the localization analysis of the protein expression in the tissue by MALDI-MSI has been applied as a general analysis method by means of the on-tissue digestion technique.[13] For small molecules, the spatial resolution, mass resolution, and scan speed of MSI were dramatically improved with the help of laser systems.[14] Following the improvement of these technologies, MALDI-MSI can be applied to medical samples and will play an important role in many fields, especially clinical diagnosis and biomarker development research.[15−18]

In fact, the MALDI-MSI technology has been applied to the analysis of drug metabolism in the whole body of a mouse,[19,20] fish,[21] and insect[22] and to the development of a determination method for drugs in biological tissues.[19] However, there remain critical issues that prevent the further development of this approach. In the process of sample preparation, the adhesive density on the surface between the cryosection and conductive materials is important for the sensitive detection of features because conductivity is required for many of the systems used for MALDI-MSI analysis, but this point still needs improvement. Conventionally, an indium tin oxide (ITO) coated glass slide is used as the conductive material on

Received: March 5, 2019
Accepted: June 18, 2019
Published: June 18, 2019

DOI: 10.1021/acs.analchem.9b01159
Anal. Chem. XXXX, XXX, XXX−XXX

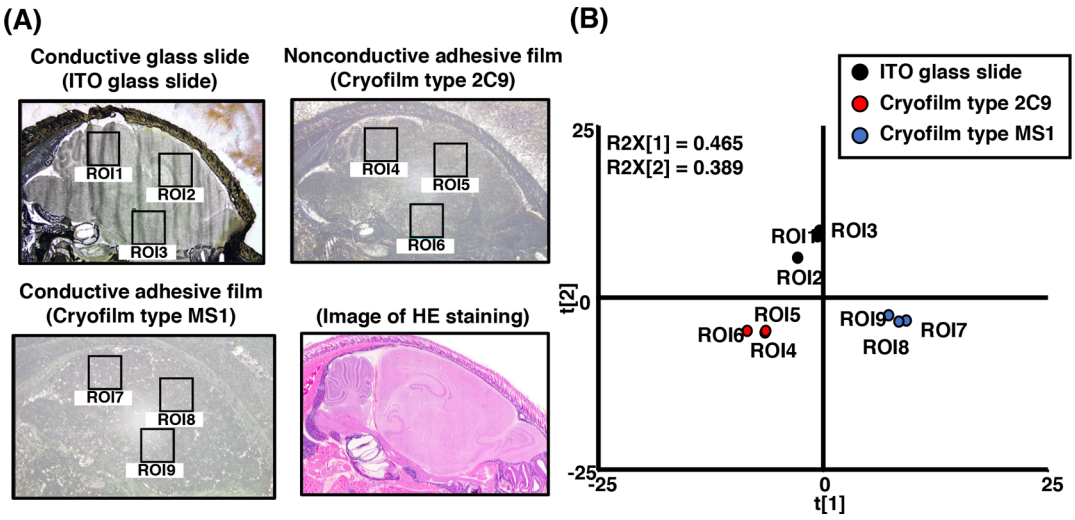

Figure 1. (A) Three typical regions of interest (ROIs) on optical images of cryosections prepared using an ITO glass slide (ROI1−3; left top panel), a nonconductive adhesive film (Cryofilm type 2C9; ROI4−6; right top panel), a conductive adhesive film (Cryofilm type MS1; ROI7−9; left bottom panel), and the image of HE staining of the analytical area of the brain (right bottom panel). (B) Score plots of principal component analysis (PCA) based on the intensity of features detected from each ROI described above. Results obtained using an ITO glass slide, a nonconductive adhesive film, and a conductive adhesive film are represented by black, red, and blue dots, respectively.

which the cryosection is set. Whereas tissue sections of the brain, liver, kidney, or heart can be prepared on a glass slide by the conventional technique, cryosections of the whole mouse body, bone, tooth, skin, lung, and fat tissues are difficult to prepare on glass slides.[23,24] To overcome this problem, an adhesive film (Cryofilm) has been introduced into the section preparation process;[25,26] high-quality frozen sections for such samples were successfully prepared.

A method utilizing a nonconductive adhesive film (Cryofilm type 2C(9)) has been applied in MALDI-MSI analyses.[27,28] However, the signal intensity from the section with the nonconductive adhesive film is lower than that from the section with the ITO glass slide because of the nonconductivity of the adhesive film.[29] To overcome this setback, we have introduced a conductive adhesive film and tested the quality and efficiency of the approach with the film.

In this study, we tried to make frozen sections from a whole mouse body with conductive adhesive films and evaluated the quality of the sections on the basis of the signal intensities of representative compounds detected by MALDI-MSI. We made frozen sections with three types of conductive adhesive tapes and films: aluminum foil tape, copper foil tape, and a conductive type of adhesive film. Of these three tapes, we succeeded in preparing high-quality frozen sections with the conductive adhesive film. The usefulness of the conductive adhesive film was evaluated by means of the signal intensities of phosphatidylcholines (PCs), which were extracted by multivariate analysis techniques, i.e., principal component analysis (PCA) and orthogonal partial least-squares-discriminant analysis (OPLS-DA), to determine the most representative compound detected by MALDI-MSI analysis. We evaluated the influence of the contact state between the cryosection and adhesive film using freeze-dried sections and thawed sections on the basis of the signal intensities of the following representative compounds in mass spectra: amino acids, cholesterol, and PCs. We have produced visualized images of the distributions of PCs and heme acquired by MALDI-MSI in five areas, including the brain, heart and liver, spleen and kidney, around the iliac body, and the testis and ileum, of the cryosections with conductive and nonconductive adhesive films.

EXPERIMENTAL SECTION

Preparation of a Cryosection of a Whole Body of a Mouse. The whole body of the mouse (ICR, male, 9 days old) was frozen in a mixture of hexane and dry ice and then freeze-embedded in embedding medium (SCEM, included in the kit) according to Kawamoto's film method. The frozen sample was set on a cryostat (CM 3050S; Leica Microsystems, Germany) and trimmed until the targeted surface appeared. Then, a frozen section (10 μm) was prepared on an ITO glass slide (100 Ω/sq; Matsunami, Osaka, Japan) as a positive control using a conventional technique for MALDI-MSI analysis. The sections for MALDI-MSI were prepared with the following adhesive films: a nonconductive adhesive film (Cryofilm type 2C9), a conductive adhesive tape consisting of copper foil, a conductive adhesive tape consisting of aluminum foil, and a conductive type of adhesive film (Cryofilm type MS1). The section was freeze-dried in the cryostat and fixed with double-sided adhesive tape on a standard glass slide. According to a conventional technique, a section was directly prepared on an ITO glass slide. A section for histological observation was prepared according to Kawamoto's method. In brief, a section (5 μm) was prepared with an adhesive film (Cryofilm type 3C16UF), stained with hematoxylin and eosin (HE), and then mounted with mounting medium (SCMM-R2, SECTION-LAB Co. Ltd.) between a glass slide and the adhesive film.

MALDI-MSI Analysis. The analytical region exposed to laser irradiation was marked under light microscopic observation. Then, a matrix (α-cyano-4-hydroxycinnamic acid, CHCA) with a thickness of 0.7 μm was deposited on the slides in a deposition system (iMLayer, Shimadzu, Kyoto, Japan), and the samples were immediately analyzed with MALDI-MSI (iMScope, Shimadzu). The conditions of MALDI-MSI analysis are shown in Table S1. The data collected through the microscopic system were digitally processed with software (Imaging MS Solution 1.30.06, Shimadzu). The compounds were identified with the MS/

DOI: 10.1021/acs.analchem.9b01159
Anal. Chem. XXXX, XXX, XXX−XXX

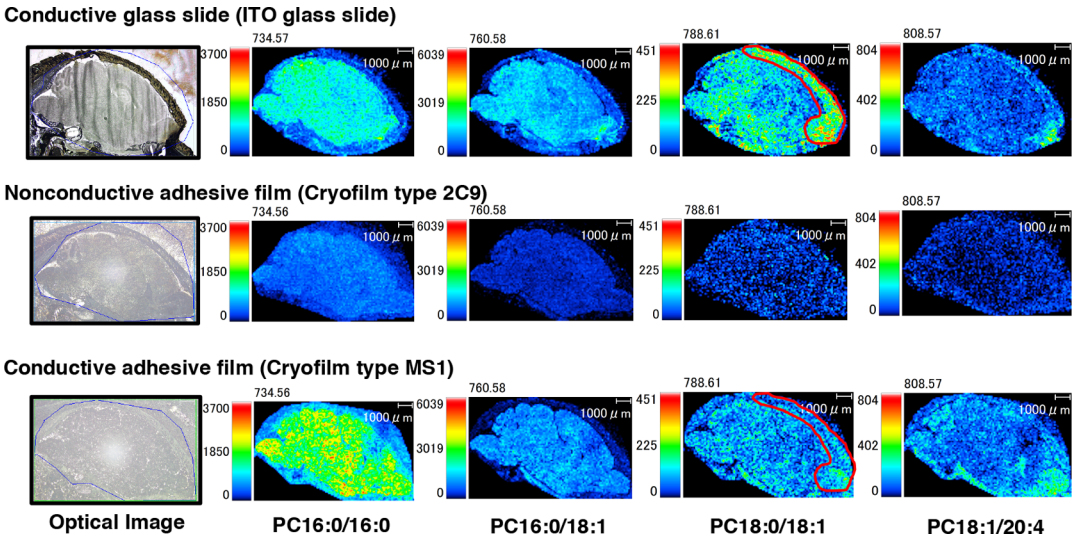

Figure 2. Optical and visualized images of phosphatidylcholines (PCs) of m/z 734.56 (PC16:0/16:0), m/z 760.58 (PC16:0/18:1), m/z 788.61 (PC18:0/18:1), and m/z 808.57 (PC18:1/20:4) in the cryosections obtained from a mouse brain on an ITO glass slide (top panels), a nonconductive adhesive film (Cryofilm type 2C9, middle panels), and a conductive adhesive film (Cryofilm type MS1, bottom panels). The intensities of the mass spectra at each spot irradiated by the laser were normalized by the maximum abundance of each compound, and the intensities are shown on the basis of the colored scale bar on the left side of the visualized images.

MS spectrum using chemical standards referenced by the identification method.[30,31]

Multivariate Data Analysis. The signal intensities of the mass spectra from commonly detected features in three typical regions of interest (ROIs) on each type of cryosection were listed by the software automatically and used for multivariate analysis. The signal intensities of the features were imported into SIMCA 13.0.0 software (Umetrics, Umeå, Sweden), and their relative quantities were evaluated by PCA and OPLS-DA.

RESULTS AND DISCUSSION

Utilization of a Conductive Adhesive Film for MALDI-MSI. An outline of the method from the sample preparation procedure to the MALDI-MSI analysis is shown in Figure S1A. The flow includes embedding, sectioning, treatment for MALDI-MSI, analysis of specific low-molecular-weight molecules, and visualization of identified metabolites. The details of the protocols are described in the Experimental Section.

Optical images of the cryosections obtained from whole bodies of mice with a nonconductive adhesive film and a conductive adhesive film are shown in Figure S1B. For this cryosection preparation, we tested three types of conductive adhesive tapes and films: i.e., aluminum foil tape, copper foil tape, and a conductive type of adhesive film. Among these tapes/films, we could prepare high-quality frozen sections with only the conductive adhesive film, while the other types of tapes/films did not allow us to prepare high-quality sections.

Conductive Adhesive Film Provides Better Signal Intensity than the Nonconductive Adhesive Film. To prepare high-quality whole body or other specific tissue cryosections, adhesive films have an advantage over the ITO glass slide. In this regard, two types of adhesive films are available: conductive and nonconductive. Therefore, we next compared the signal intensities of the cryosections obtained by using the conductive and nonconductive adhesive films. Figure 1A shows optical images of three typical ROIs, each of which is from cryosections of the whole body and the area corresponding to the brain. In this analysis, we used an ITO glass slide (left top panel; ROI1−3), a nonconductive adhesive film (Cryofilm type 2C9) (right top panel; ROI4−6), which was used in the previous studies for MALDI-MSI analysis, and a conductive adhesive film (Cryofilm type MS1) (left bottom panel; ROI7−9). While the ITO glass slide is traditionally and widely used for the MALDI-MSI analysis, the handling of the cryosections is much easier when adhesive films are used. We also give the signal intensities of 100 commonly detected features in the mass spectra from the sections corresponding to the ITO glass slide and adhesive films in Table S2.

Our next concern is whether good-quality signals could be obtained with the use of adhesive films. The PCA score plot clearly demonstrates a large variation among the three groups (Figure 1B). To assess the quality of the signals with the use of adhesive films, we next conducted *S*-plot analyses by means of OPLS-DA. First, we compared the signals of the sections on the nonconductive adhesive film with those on the ITO glass slide. We found that 24 features extracted from the *S*-plot were lower in abundance on the nonconductive film than on the ITO glass slide (Figure S2A). Those features were selected on the basis of $p(\mathrm{corr})[1]$ being greater than 0.9 or less than −0.9 and $p[1]$ being greater than 0.1 or less than −0.1, which was derived from the *S*-plot analysis with separation based on larger changes in their abundance between the two types of cryosection.

Second, we compared signals of the sections on the conductive adhesive film with those on the nonconductive adhesive film. We found that 29 extracted features of the former were higher in abundance than in the latter (Figure S2B), indicating that the conductive adhesive film gives rise to higher-quality signals in comparison to those of the nonconductive adhesive film. To verify this result, we then compared the signals of sections from the conductive adhesive film with those of sections on the ITO glass slide. We found that 16 and 8 similarly extracted features were higher and lower in abundance with the use of the conductive adhesive film in comparison to that with the ITO glass slide, respectively (Figure S2C).

DOI: 10.1021/acs.analchem.9b01159
Anal. Chem. XXXX, XXX, XXX−XXX

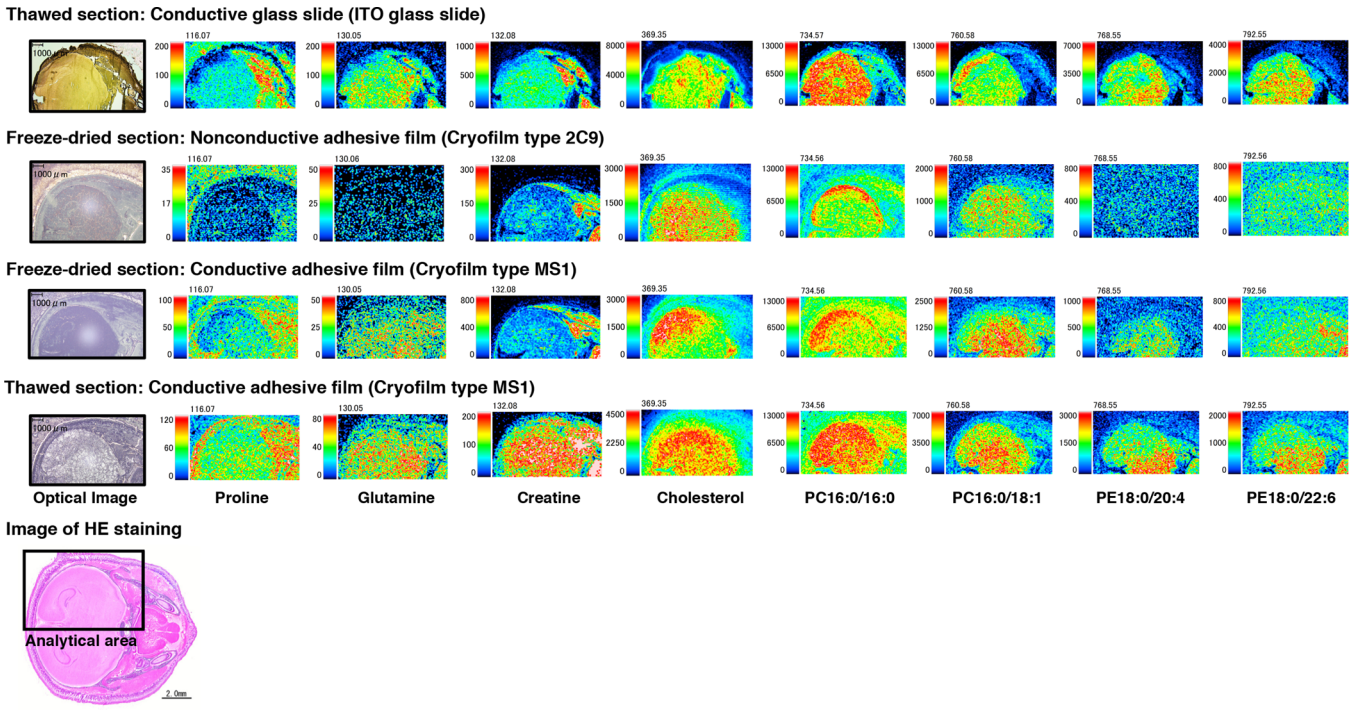

Figure 3. Optical and visualized images of compounds detected by MALDI-MSI analyses on cryosections obtained from a mouse brain. Visualized images of compounds are *m/z* 116.07 (proline), *m/z* 130.05 (glutamine), *m/z* 132.08 (creatine), *m/z* 369.35 (cholesterol), *m/z* 734.57 (PC16:0/16:0), *m/z* 760.58 (PC16:0/18:1), *m/z* 768.55 (PE18:0/20:4), and *m/z* 792.55 (PE18:0/22:6). The visualized images were normalized by the absolute intensity to maximize the contrast in each image. The image of HE staining of the analytical area of the brain is shown beneath the visualized images. The nonconductive adhesive film and conductive adhesive film were Cryofilm type 2C9 and Cryofilm type MS1, respectively.

A list of the identified compounds in these analyses, which excluded ions derived from the matrix or isotopes, is shown in Table S3. We clearly detected signals of PCs and phosphatidylethanolamines (PEs) in the mass spectra, as has been reported in the analyses of mouse brain sections by MALDI-MSI.[32−34] The majority of the PCs and PEs were significantly lower in abundance when a nonconductive adhesive film was used, while in contrast, the PCs were significantly higher in abundance when the conductive adhesive film was used; however, the signals of the PEs and sphingomyelin were still lower even when the adhesive film was conductive.

The differences in signal intensity were derived from the material. The conductive adhesive film evenly included carbon particles in the cryofilm. The images of the structure of cryosections on the ITO glass slide, nonconductive adhesive film (Cryofilm type 2C9), and conductive adhesive film (Cryofilm type MS1) are shown in Figure S3. Although the metals have better conductivity than carbon, the flexibility and solubility are also important to include in the cryofilm to keep the strength of adhesive power. We examined several metals, but they did not allow us to prepare high-quality sections described above. In addition, the carbon rate in the film can be optimized to maintain the adhesive power and conductivity. Therefore, we finally concluded that carbon was better to create the high-quality cryosection for MALDI-MSI.

Images of Sections on Conductive and Nonconductive Adhesive Films. We then examined optical and visualized images of the representative PCs. As shown in Figure 2, PCs of *m/z* 734.56 (PC16:0/16:0), *m/z* 760.58 (PC16:0/18:1), *m/z* 788.61 (PC18:0/18:1), and *m/z* 808.57 (PC18:1/20:4) in the cryosections obtained from a mouse brain on an ITO glass slide (top panels), a nonconductive adhesive film (middle panels), and a conductive adhesive film (bottom panels) were detected and compared.

In the visualized images, the relative intensities of the PCs were significantly higher in the mass spectra acquired from the cryosection using the conductive adhesive film than in those acquired from the cryosection using the nonconductive adhesive film (Figure 2).

The absolute intensities of the MALDI-MSI mass spectra from a representative area on the mouse brain cryosection prepared using an ITO glass slide, nonconductive adhesive film, and conductive adhesive film are shown in Figure S4A. The maximum intensities were 1.7×10^6, 7.0×10^5 and 2.6×10^6, respectively. Thus, the signal intensity of PC16:0/16:0 obtained using the conductive adhesive film was 3.8 times higher than that obtained using the nonconductive adhesive film and 1.5 times higher than that obtained using the ITO glass slide.

The localization of the PCs (typically PC16:0/18:1) at the boundary of the brain was clearer on the magnified images acquired using the conductive adhesive film than in those acquired using the ITO glass slides (Figure S4B). However, the visualized images of PC16:0/18:1 at the cranium area between the ITO glass slide and films had some differences. Recent studies have indicated the importance of combinatory examinations incorporating both a meticulous distribution analysis by MALDI-MSI and an elaborate determination analysis by high-performance liquid chromatography mass spectrometry (LC-MS).[35−38] A combinatory use of the adhesive films for the laser microdissection (LMD) approach may give rise to a solution for this issue. We then detected PC16:0/18:1 by LC-MS in the specific cranium and cortex

DOI: 10.1021/acs.analchem.9b01159
Anal. Chem. XXXX, XXX, XXX−XXX

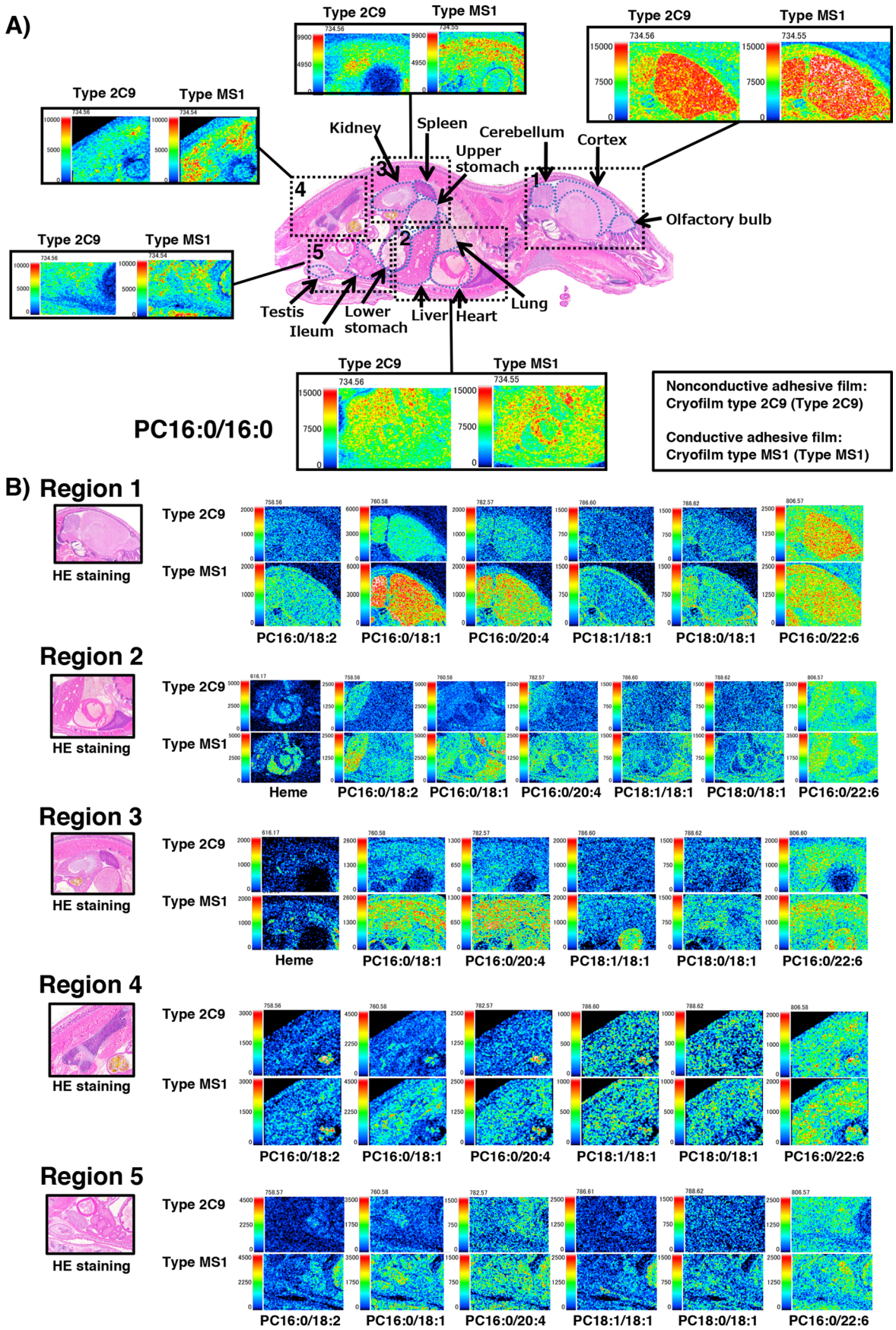

Figure 4. (A) Optical images of cryosections obtained from the whole body of a mouse with hematoxylin and eosin (HE) staining and images visualized by signal intensity of *m/z* 734.56 (PC16:0/16:0) in five areas: brain (region 1), heart and liver (region 2), kidney and spleen (region 3), around the iliac body (region 4), and testis and ileum (region 5). Note that the representative areas in region 1 (brain) as well as in regions 2, 3,

DOI: 10.1021/acs.analchem.9b01159
Anal. Chem. XXXX, XXX, XXX−XXX

Figure 4. continued

and 5 are marked by dotted blue lines. (B) HE staining and visualized images of compounds m/z 760.58 (PC16:0/18:1), m/z 758.56 (PC16:0/18:2), m/z 782.57 (PC16:0/20:4), m/z 806.57 (PC16:0/22:6), m/z 788.62 (PC18:0/18:1), m/z 786.60 (PC18:1/18:1), and m/z 616.17 (heme) on cryosections prepared using nonconductive (Cryofilm type 2C9) and conductive adhesive films (Cryofilm type MS1) in the five areas (regions 1−5). The relative intensities in the visualized images were normalized by the highest signal of each compound, which was detected on the cryosection obtained from the nonconductive or conductive adhesive film at each region and is shown in red on the color coding in the left bar.

area of the brain section by the LMD system following the approach of a previous report.[37] We found that the signals from the cranium area were 10 times lower than that from the cortex by the LC-MS analysis (Figure S5A). The difference in signal intensity of MALDI-MSI was matched to the conductive adhesive film (Cryofilm type MS1) (Figure S5B). Some metabolites are unstable in the cryosection and quickly changed during the thawing periods, even if we kept the manipulation over a very short period, as the process of enzyme reaction or degradation of phosphate groups might occur in these periods. Our results indicate that PC16:0/18:1 is one of the unstable metabolites increasing under the freeze−thawed condition and easily gives rise to an artifact.

Freeze-Dried Sections with or without Freeze−Thawing. To assess the freeze−thaw effect of the cryosections on the signal intensities of the MALDI-MSI analysis, we prepared cryosections with nonconductive and conductive adhesive films. The sections with the films were divided into two groups. One group of sections was completely freeze-dried in the cryostat, and the other was thawed by removing the section from the cryostat. The adhesive films with the sections were fixed on a glass slide with double-sided adhesive tape. The optical images and visualized images of representative compounds detected in the scan range from m/z 100 to 900 by MALDI-MSI analyses on the cryosections obtained from a mouse brain are shown in Figure 3.

In the visualized images, the relative intensities of representative compounds on the cryosections, such as m/z 116.07 (proline), m/z 130.05 (glutamine), m/z 132.08 (creatine), m/z 369.35 (cholesterol), m/z 734.57 (PC16:0/16:0), m/z 760.58 (PC16:0/18:1), m/z 768.55 (PE18:0/20:4) and m/z 792.55 (PE18:0/22:6), were significantly reduced when the nonconductive adhesive film was used for the freeze-dried sections in comparison to those when the ITO glass slide was used for the thawed sections (Figure 3, top panels vs the second-row panels). Although the visualized images were improved by using a conductive adhesive film for the freeze-dried sections (the third-row panels), the intensities were still lower than those obtained using the ITO glass slide.

We then compared the difference in signal intensities between the cryosections that were immediately freeze-dried and those that were thawed once before freeze-drying. We found that the signal intensities in the visualized images appeared to be higher in the cryosections thawed once before freeze-drying than in the cryosection immediately freeze-dried (the third-row panels vs bottom panels).

In the MALDI-MSI analysis using ITO glass slides the cryosections are usually thawed once to transmit their conductivity. On the other hand, with the use of adhesive films, the cryosections had no need to be melted for staining or other observation analyses. This highlights an important issue regarding the tradeoff relationship between the quality of the tissue images and the high output of the signals. Although the sensitivity was improved using the conductive adhesive films once thawed before freeze-drying, as the sections were tightly contacted to the adhesive surface by the thawing, the localization information on the compounds in the tissues became obscure or was changed when the cryosection was thawed once, as seen in our current analyses and as also has been reported.[25,26] Therefore, we concluded that the cryosections should be thawed to obtain the higher sensitivity of stable metabolites or immediately freeze-dried to obtain an accurate distribution and correct information for unstable metabolites after cutting the cryosections with the conductive adhesive film.

Whole-Body Analysis. One of the important advantages that the adhesive films confer to the MALDI-MSI analysis is the improvement of the cryosection preparation of a whole body. To assess whether conductive adhesive films give rise to better support than do nonconductive adhesive films, we prepared three serial whole-body sections. The first section (5 μm thickness) was stained with HE for identifying tissues, and the other two sections (10 μm thickness) were used for the MALDI-MSI analyses.

As shown in Figure 4A, five areas in the whole body of a 9-day-old mouse, including the brain (region 1), heart and liver (region 2), spleen and kidney (region 3), iliac body (region 4), and testis and ileum (region 5), were analyzed by MALDI-MSI. The visualized images of the most abundant compound, m/z 736.56 (PC16:0/16:0), detected on the cryosections prepared using the nonconductive and conductive adhesive films are shown side by side (left and right panels, respectively). The relative intensities of the PC16:0/16:0 in all five areas were significantly increased on the cryosection prepared using the conductive adhesive film. While this analysis unequivocally highlighted the abundant expression of PC16:0/16:0 in the brain, the localization of this PC in the other regions was much clearer on the conductive adhesive film than on the nonconductive adhesive film, especially on the edges and boundaries around the organs.

Then, we focused on representative compounds, namely, m/z 758.56 (PC16:0/18:2), m/z 760.58 (PC16:0/18:1), m/z 782.57 (PC16:0/20:4), m/z 786.60 (PC18:1/18:1), m/z 788.60 (PC18:0/18:1), m/z 806.55 (PC16:0/22:6), and m/z 616.17 (heme, only in regions 2 and 3), detected with high abundance in the five areas on the cryosections to evaluate the effect of the conductivity and obtained HE staining and visualized images of these compounds by MALDI-MSI analyses (Figure 4B).

In the brain of region 1, all PCs were detected at high levels on the cryosection prepared with the conductive adhesive film. Importantly, their distributions were clearly observed: PC16:0/18:1 and PC16:0/20:4 were localized in the cortex and cerebellum, while PC18:0/18:1 and PC18:1/18:1 were localized in the olfactory bulb and around the skull and cerebellum.

Similarly, in the heart and liver of region 2, all species of PCs and heme were detected at high levels on the cryosection prepared with the conductive adhesive film, and their distributions were also clearly observed. PC16:0/16:0 and

DOI: 10.1021/acs.analchem.9b01159
Anal. Chem. XXXX, XXX, XXX−XXX

PC16:0/18:1 were highly localized in the lung, whereas lower signals were observed for PC16:0/20:4 and PC16:0/22:6 in this area. The saturated fatty acid and monounsaturated fatty acid levels were higher than the polyunsaturated fatty acid levels because there are oxidized fatty acids in the lung that defend against the effects of oxidization resulting from peroxidation by oxygen.[39] Our results are consistent with those from a previous report about the difference in fatty acid species in the lung.[40] PC16:0/18:2 was localized in the liver and not in the other organs in region 2, and many species of PCs were localized in the muscle area of the heart. In contrast, heme was highly detected in the blood area of the heart.

In the spleen and kidney of region 3, high levels of all PCs and heme were detected on the cryosection prepared with the conductive adhesive film, and their distributions were clearly observed. The localization of heme in the spleen was clear, and high levels of the PCs were detected in the kidney area. In addition, the levels of PCs detected in the upper stomach area were very clear, especially PC18:1/18:1, when the conductive adhesive film was used.

Around the iliac body of region 4, higher levels of PC16:0/18:1, PC16:0/18:2, PC16:0/20:4, and PC16:0/22:6 were detected on the cryosection prepared with the conductive adhesive film in comparison to those prepared with the nonconductive adhesive film. Their localizations were similar to those of the image taken using nonconductive adhesive film.

At the testis and ileum of region 5, all PCs were highly detected on the cryosection prepared with the conductive adhesive film, and their distributions were clearly observed. The localization of PC16:0/18:1 was observed in the testis and ileum area when the conductive adhesive film was used, and many PCs could be detected in the ileum and lower stomach area. These results thus demonstrate that the conductive adhesive film is useful for the sensitive detection and clear visualization of the distribution of biological compounds by MALDI-MSI analysis.

Advantages and Future of the Conductive Adhesive Film. A number of analyses of the whole mouse body or other creatures by MALDI-MSI have been reported previously.[21−23,29] However, one critical issue that needed to be overcome that prevented the further use of this procedure is that most of the cryosections in those studies could not maintain their form or structure, even though their findings on the localization of compounds had a strong impact. Although cryosections of soft tissues or organs can easily be prepared and set on ITO glass slides via a conventional method for MALDI-MSI analysis, this method cannot be applied to hard tissues, such as bone, tooth, skin, muscle, entire head parts, whole mouse embryos, and whole bodies. The method is also not applicable for fragile tissues, including the lung and fat, which are morphologically distorted easily and/or drop off easily during the cutting processes or pasting onto the glass slides. In contrast, the conductive adhesive film is able to provide a high-quality cryosection for any tissue or biological material, as shown in the above results, by maintaining their form/structure and cell localization.

The methods using double-sided tape with conductivity for MALDI-MSI analysis[41] and the application of whole-body imaging by the double-sided tape with conductive tape have been reported.[42] Similarly, a double-sided tape with gold deposition for conductivity has also been reported.[43] Although the sample plate for MALDI-MSI analysis has conductivity using such kinds of double-sided tapes, the charged substances that were produced from the section could not be efficiently removed during the MALDI analysis. The direct contact with conductive material more efficiently removed the charged substances and improved the signal intensity. The conductive adhesive film utilized here includes the carbon particle in the cryofilm and the conductive particles were in direct contact on the surface of the cryosection (Figure S3). The conductive adhesive film can be used for a simple and reproducible process to create cryosections for MALDI-MSI analysis. Although the deposition of gold on the cryosection could result in better signal intensity,[43] it should also be noted that the optimization of the thickness of gold layer is technically difficult even by LDI-MSI, as the surface of gold deposition may have some clusters with matrix on the cryosection and reduce the reliability of their distribution.[44,45]

Whereas the signals from the materials used for embedding a frozen sample often interfere with those from the targeted compound, no such signals corresponding to the embedding medium (SCEM) could be detected in the tissue areas of the sections on the conductive adhesive film. Additionally, the noise levels of mass spectra in each region 1−5 between the nonconductive and conductive adhesive films appeared to be similar, and the signal intensities of mass spectra from compounds on the conductive adhesive film were clearly higher. The conductive adhesive film thus succeeds in the significant reduction of the interfering signal intensity and gives higher signals without increasing the noise of the background, which is useful for MALDI-MSI analysis.

One disadvantage of the conductive adhesive film method is that the cryosections with the film cannot be examined by routine light microscopy, because the film appears opaque using carbon particles. However, this point can be overcome with the preparation of continuous cryosections with the conductive adhesive film (Cryofilm type MS) and other types of Cryofilm such as Cryofilm type 3C(16UF) successively. The latter will be rendered for the HE staining or other immunostaining methods that identify the distribution of tissues and cells in the analytical area by MALDI-MSI analysis.

CONCLUSIONS

In the present study, we evaluated the effect of a conductive adhesive film on the visualized images of representative biological compounds. We demonstrated that the conductive adhesive film can overcome the setbacks of the MALDI-MSI approach by allowing the imaging of intact cryosections. The conductive adhesive film is a powerful tool for MALDI-MSI analysis, as the film is able to produce high-quality frozen sections with minimal technical difficulties.

ASSOCIATED CONTENT

Supporting Information

The Supporting Information is available free of charge on the ACS Publications website at DOI: 10.1021/acs.analchem.9b01159.

Experimental details and figures and tables as described in the text (PDF)

AUTHOR INFORMATION

Corresponding Authors

*D.S.: tel, +81-22-274-5925; fax, +81-22-274-5930; e-mail, saigusa@m.tohoku.ac.jp.

DOI: 10.1021/acs.analchem.9b01159
Anal. Chem. XXXX, XXX, XXX−XXX

*T.K.: tel, +81- 45-580-8448; e-mail, kawamoto-t@tsurumi-u.ac.jp.

ORCID

Daisuke Saigusa: 0000-0001-9484-9870

Notes

The authors declare no competing financial interest.

■ ACKNOWLEDGMENTS

This investigation was supported by the LEAP from the Japan Agency for Medical Research and Development (AMED) (J19gm0010004) and a Grant-In-Aid from the Japan Society for the Promotion of Society (K17K08233). This work was also supported in part by the Tohoku Medical Megabank Project through the Ministry of Education, Culture, Sports, Science and Technology of Japan, by the Reconstruction Agency of Japan, and by the Japan AMED (JP19km0105001 and JP19km0105002). The funders had no role in the study design, data collection and analysis, decision to publish, or preparation of the manuscript.

■ REFERENCES

(1) Spengler, B. *Anal. Chem.* **2015**, *87* (1), 64−82.
(2) Shimma, S.; Sugiura, Y.; Hayasaka, T.; Matsumoto, M.; Setou, M. *Anal. Chem.* **2008**, *80*, 878−885.
(3) Boughton, B. A.; Thinagaran, D.; Sarabia, D.; Bacic, A.; Roessner, U. *Phytochem. Rev.* **2016**, *15*, 445−488.
(4) Qin, L.; Zhang, Y.; Liu, Y.; He, H.; Han, M.; Li, Y.; Zeng, M.; Wang, X. *Phytochem. Anal.* **2018**, *29* (4), 351−364.
(5) Khalil, S. M.; Römpp, A.; Pretzel, J.; Becker, K.; Spengler, B. *Anal. Chem.* **2015**, *87* (22), 11309−11316.
(6) Sugiura, Y.; Shimma, S.; Setou, M. *Anal. Chem.* **2006**, *78* (24), 8227−8235.
(7) Shimma, S.; Takashima, Y.; Hashimoto, J.; Yonemori, K.; Tomura, K.; Hamada, A. *J. Mass Spectrom.* **2013**, *48* (12), 1285−1290.
(8) Shimma, S.; Sugiura, Y. *Mass Spectrom. (Tokyo)* **2014**, *3*, S0029.
(9) Nakamura, J.; Morikawa-Ichinose, T.; Fujimura, Y.; Hayakawa, E.; Takahashi, K.; Ishii, T.; Miura, D.; Wariishi, H. *Anal. Bioanal. Chem.* **2017**, *409* (6), 1697−1706.
(10) Sugiyama, E.; Masaki, N.; Matsushita, S.; Setou, M. *Anal. Chem.* **2015**, *87* (22), 11176−11181.
(11) Shimma, S.; Kumada, H. O.; Taniguchi, H.; Konno, A.; Yao, I.; Furuta, K.; Matsuda, T.; Ito, S. *Anal. Bioanal. Chem.* **2016**, *408* (27), 7607−7615.
(12) Sugiura, Y.; Konishi, Y.; Zaima, N.; Kajihara, S.; Nakanishi, H.; Taguchi, R.; Setou, M. *J. Lipid Res.* **2009**, *50* (9), 1776−1788.
(13) Ryan, D. J.; Spraggins, J. M.; Caprioli, R. M. *Curr. Opin. Chem. Biol.* **2019**, *48*, 64−72.
(14) Yoon, S.; Lee, T. G. *Nano Converg.* **2018**, *5* (1), 24.
(15) Michno, W.; Kaya, I.; Nyström, S.; Guerard, L.; Nilsson, K. P. R.; Hammarström, P.; Blennow, K.; Zetterberg, H.; Hanrieder, J. *Anal. Chem.* **2018**, *90* (13), 8130−8138.
(16) Hong, J. H.; Kang, J. W.; Kim, D. K.; Baik, S. H.; Kim, K. H.; Shanta, S. R.; Jung, J. H.; Mook-Jung, I.; Kim, K. P. *J. Lipid Res.* **2016**, *57* (1), 36−45.
(17) Stark, D. T.; Anderson, D. M. G.; Kwong, J. M. K.; Patterson, N. H.; Schey, K. L.; Caprioli, R. M.; Caprioli, J. *Invest. Ophthalmol. Visual Sci.* **2018**, *59* (1), 212−222.
(18) Sato, K.; Saigusa, D.; Saito, R.; Fujioka, A.; Nakagawa, Y.; Nishiguchi, K. M.; Kokubun, T.; Motoike, I. N.; Maruyama, K.; Omodaka, K.; Shiga, Y.; Uruno, A.; Koshiba, S.; Yamamoto, M.; Nakazawa, T. *Sci. Rep.* **2018**, *8*, 11930.
(19) Castellino, S.; Groseclose, M. R.; Wagner, D. *Bioanalysis* **2011**, *3* (21), 2427−2441.
(20) Karlsson, O.; Hanrieder, J. *Arch. Toxicol.* **2017**, *91* (6), 2283−2294.
(21) Nelson, K. A.; Daniels, G. J.; Fournie, J. W.; Hemmer, M. J. *J. Biomol. Technol.* **2013**, *24* (3), 119−127.
(22) Ohtsu, S.; Yamaguchi, M.; Nishiwaki, H.; Fukusaki, E.; Shimma, S. *Anal. Sci.* **2018**, *34* (9), 991−996.
(23) Trim, P. J. *Methods Mol. Biol.* **2017**, *1618*, 175−189.
(24) de Macedo, C. S.; Anderson, D. M.; Schey, K. L. *Talanta* **2017**, *174*, 325−335.
(25) Kawamoto, T. *Arch. Histol. Cytol.* **2003**, *66* (2), 123−143.
(26) Kawamoto, T.; Kawamoto, K. *Methods Mol. Biol.* **2014**, *1130*, 149−164.
(27) Fujino, Y.; Minamizaki, T.; Yoshioka, H.; Okada, M.; Yoshiko, Y. *Bone Rep.* **2016**, *5*, 280−285.
(28) Hirano, H.; Masaki, N.; Hayasaka, T.; Watanabe, Y.; Masumoto, K.; Nagata, T.; Katou, F.; Setou, M. *Anal. Bioanal. Chem.* **2014**, *406* (5), 1355−1363.
(29) Prideaux, B.; Stoeckli, M. *J. Proteomics* **2012**, *75* (16), 4999−5013.
(30) Palmer, A.; Phapale, P.; Chernyavsky, I.; Lavigne, R.; Fay, D.; Tarasov, A.; Kovalev, V.; Fuchser, J.; Nikolenko, S.; Pineau, C.; Backer, M.; Alexandrov, T. *Nat. Methods.* **2017**, *14* (1), 57−60.
(31) Hartler, J.; Triebl, A.; Ziegl, A.; Trötzmüller, M.; Rechberger, N. G.; Zeleznik, A. O.; Zierler, A. K.; Torta, F.; Cazenave-Gassiot, A.; Wenk, R. M.; Fauland, A.; Wheelock, E. C.; Armando, M. A.; Quehenberger, O.; Zhang, Q.; Wakelam, O. J. M.; Haemmerle, G.; Spener, F.; Köfeler, C. H.; Thallinger, G. G. *Nat. Methods* **2017**, *14* (12), 1171−1174.
(32) Jackson, S. N.; Wang, H. Y.; Woods, A. S. *Anal. Chem.* **2005**, *77*, 4523−4527.
(33) Murphy, R. C.; Hankin, J. A.; Barkley, R. M. *J. Lipid Res.* **2009**, *50* (Suppl), S317−22.
(34) Hankin, J. A.; Farias, S. E.; Barkley, R. M.; Heidenreich, K.; Frey, L. C.; Hamazaki, K.; Kim, H. Y.; Murphy, R. C. *J. Am. Soc. Mass Spectrom.* **2011**, *22*, 1014−1021.
(35) Jones, E. E.; Zhang, W.; Zhao, X.; Quiason, C.; Dale, S.; Shahidi-Latham, S.; Grabowski, G. A.; Setchell, K. D. R.; Drake, R. R.; Sun, Y. *SLAS Discovery* **2017**, *22* (10), 1218−1228.
(36) Matsumoto, J.; Sugiura, Y.; Yuki, D.; Hayasaka, T.; Goto-Inoue, N.; Zaima, N.; Kunii, Y.; Wada, A.; Yang, Q.; Nishiura, K.; Akatsu, H.; Hori, A.; Hashizume, Y.; Yamamoto, T.; Ikemoto, K.; Setou, M.; Niwa, S. *Anal. Bioanal. Chem.* **2011**, *400*, 1933−1943.
(37) Yagishita, Y.; Uruno, A.; Fukutomi, T.; Saito, R.; Saigusa, D.; Pi, J.; Fukamizu, A.; Sugiyama, F.; Takahashi, S.; Yamamoto, M. *Cell Rep.* **2017**, *18* (8), 2030−2044.
(38) Sato, E.; Saigusa, D.; Mishima, E.; Uchida, T.; Miura, D.; Morikawa-Ichinose, T.; Kisu, K.; Sekimoto, A.; Saito, R.; Oe, Y.; Matsumoto, Y.; Tomioka, Y.; Mori, T.; Takahashi, N.; Sato, H.; Abe, T.; Niwa, T.; Ito, S. *Toxins (Basel)* **2018**, *10* (1), 19.
(39) Nakamura, A.; Ebina-Shibuya, R.; Itoh-Nakadai, A.; Muto, A.; Shima, H.; Saigusa, D.; Aoki, J.; Ebina, M.; Nukiwa, T.; Igarashi, K. *J. Exp. Med.* **2013**, *210* (11), 2191−2204.
(40) Postle, A. D.; Gonzales, L. W.; Bernhard, W.; Clark, G. T.; Godinez, M. H.; Godinez, R. I.; Ballard, P. L. *J. Lipid Res.* **2006**, *47*, 1322−1331.
(41) Stoeckli, M.; Farmer, T. B.; Caprioli, R. M. *J. Am. Soc. Mass Spectrom.* **1999**, *10* (1), 67−71.
(42) Khatib-Shahidi, S.; Andersson, M.; Herman, J. L.; Gillespie, T. A.; Caprioli, R. M. *Anal. Chem.* **2006**, *78* (18), 6448−6456.
(43) Stoeckli, M.; Staab, D.; Schweitzer, A. *Int. J. Mass Spectrom.* **2007**, *260*, 195−202.
(44) Dufresne, M.; Patterson, N. H.; Lauzon, N.; Chaurand, P. *Adv. Cancer Res.* **2017**, *134*, 67−84.
(45) Ràfols, P.; Vilalta, D.; Torres, S.; Calavia, R.; Heijs, B.; McDonnell, L. A.; Brezmes, J.; Del Castillo, E.; Yanes, O.; Ramírez, N.; Correig, X. *PLoS One* **2018**, *13* (12), No. e0208908.

DOI: 10.1021/acs.analchem.9b01159
Anal. Chem. XXXX, XXX, XXX−XXX